Comprehensive kinetic analysis of the plasma-wall transition layer in a strongly tilted magnetic field

D. D. Tskhakaya, Sr.[1,a)] and L. Kos[2]
[1]Institute for Theoretical Physics, Fusion@ÖAW, University of Innsbruck, A-6020 Innsbruck, Austria
[2]LECAD Laboratory, Faculty of Mech. Eng., University of Ljubljana, SI-1000 Ljubljana, Slovenia

(Received 8 September 2014; accepted 20 October 2014; published online 29 October 2014)

The magnetized plasma-wall transition (MPWT) layer at the presence of the obliquity of the magnetic field to the wall consists of three sub-layers: the Debye sheath (DS), the magnetic pre-sheath (MPS), and the collisional pre-sheath (CPS) with characteristic lengths λ_D (electron Debye length), ρ_i (ion gyro-radius), and ℓ (the smallest relevant collision length), respectively. Tokamak plasmas are usually assumed to have the ordering $\lambda_D \ll \rho_i \ll \ell$, when the above-mentioned sub-layers can be distinctly distinguished. In the limits of $\varepsilon_{Dm}(\lambda_D/\rho_i) \to 0$ and $\varepsilon_{mc}(\rho_i/\ell) \to 0$ ("asymptotic three-scale (A3S) limits"), these sub-layers are precisely defined. Using the smallness of the tilting angle of the magnetic field to the wall, the ion distribution functions are found for three sub-regions in the analytic form. The equations and characteristic length-scales governing the transition (intermediate) regions between the neighboring sub-layers (CPS – MPS and MPS – DS) are derived, allowing to avoid the singularities arising from the $\varepsilon_{Dm} \to 0$ and $\varepsilon_{mc} \to 0$ approximations. The MPS entrance and the related kinetic form of the Bohm–Chodura condition are successfully defined for the first time. At the DS entrance, the Bohm condition maintains its usual form. The results encourage further study and understanding of physics of the MPWT layers in the modern plasma facilities. © *2014 AIP Publishing LLC*.
[http://dx.doi.org/10.1063/1.4900765]

I. INTRODUCTION

The situations where a magnetic field intersects the solid wall at a small angle is rather common in plasma physics. For instance at the divertor plate of the tokamak, where the knowledge of the structure of the magnetized plasma-wall transition (MPWT) layer is necessary to reduce the undesirable fluxes to the wall.[1] At some surfaces of spacecrafts moving in the earth magnetic field as well as in the laboratory gas discharge tube (where the magnetic field is used for plasma isolation from the tube-walls), the grazing intersection angle inevitably occurs. For the tilting angle of the magnetic field lines below, we use the values $\alpha < 5^\circ$ (or $\alpha < 0.087$), which are usually assumed when considering the similar boundary layer problems in magnetized plasmas. The fluid model is not suitable for describing the MPWT layer because of the occurrence of strong inhomogeneities there. But the point is that there is little information on the kinetics of MPWT layer (especially in the analytic form) in systems where the ions' transport to the wall is strongly impeded by the tilted magnetic field.[2–4] In Ref. 4, where the kinetic problem is considered most consistently, only the so-called magnetic pre-sheath (MPS) (a sub-layer of the MPWT) is discussed, assuming it to be collisional—the charge-exchange collisions of ions with the neutrals are taken into consideration. The ion gyro-radius ρ_i is of order/less of the relevant collision length ℓ, and the width of the Debye sheath (DS) is negligibly small, $\lambda_D \to 0$. In Ref. 4, the ion distribution function, as a solution of the ion Boltzmann equation, is constructed by means of the special method using the summation over the initial conditions in the collisions. The ion density and the self-consistent electric potential further are found numerically.

To our knowledge, the present paper is a first attempt to embrace the whole MPWT layer considering its all sub-layers in the analytic form. The smallness of the inclination angle α allows to seek the ion distribution function in the form of expansion and formulates the necessary boundary conditions at the interfaces of the neighboring MPWT sub-layers.

In the presence of an oblique magnetic field, the plasma-wall transition (PWT) layer can be divided into three regions (Fig. 1), namely: the DS, the MPS, and the collision pre-sheath (CPS) with characteristic length scales λ_D, ρ_i, and ℓ, (relevant collision length), respectively.[1] For the limiting

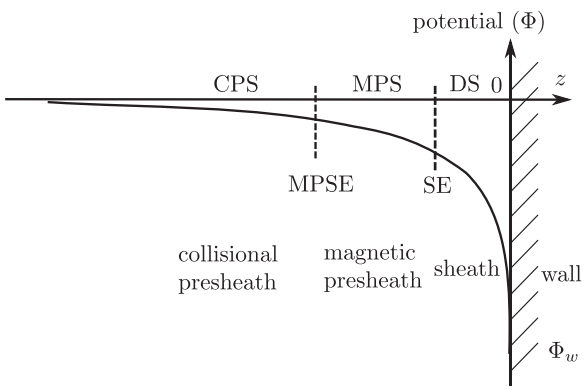

FIG. 1. Structure of the MPWT.

[a)]Also at Institute of Physics, Georgian Academy of Sciences, 0177 Tbilisi, Georgia

ordering $\lambda_D \ll \rho_i \ll \ell$ ("asymptotic three-scale (A3S) limit"), i.e., for $\varepsilon_{Dm} = (\lambda_D/\rho_i) \to 0$ and $\varepsilon_{cm} = (\rho_i/\ell) \to 0$, the DS can be characterized as collisionless and non-neutral ($n_i \neq n_e$ with n_i and n_e the ion and electron number densities, respectively), the MPS as quasi-neutral ($n_i = n_e$) and collisionless (in contrast with the consideration of Ref. 4) and the CPS as collisional and quasi-neutral.[5] In the classical PWT problem without magnetic field, the spatial monotonicity of the electric potential requires the fulfillment of the non-marginal Bohm condition at the DS interface. Chodura[5] was the first to investigate the quasineutral MPS in the fluid approximation with an oblique magnetic field without any collision effects, i.e., in the A3S limit.

The problems similar to ones presented in the paper at hand were considered numerically in Refs. 6–9. In Ref. 6, the gyro-conversion and the resulting deformation of the ion distribution function at approaching the wall are considered. The authors numerically investigate the collisionless magnetic pre- sheath and Debye sheath by applying the 4D version of the Eulerian Vlasov code (with one space and three velocity coordinates), which solves the Vlasov equation consistently with Poissons equation for a 1D structure of the electric field perpendicular to the wall. From the beginning, the ion temperature is assumed to be equal or larger than electron one. The velocity distribution function (VDF) for ions is chosen in the form of the shifted Maxwellian with the smoothing factor, which depends on the velocity along the magnetic field. The shapes of the ion distribution function, the electric potential, and the ion current densities are determined. In Ref. 7, also the Vlasov code is used to investigate the possibility of the smooth transition between an absorbing wall and a plasma in the presence of a titled magnetic field. Only two sub-layers—the magnetic pre-sheath and the Debye sheath are considered. The angle between the magnetic field and the wall is assumed not to be small. Electrons are assumed to follow the Boltzmann distribution and the ion kinetics is described by means of the Batnagar–Gross–Krook equation. It is found that the shape of the ion velocity function near the wall is far from the Maxwellian, though at the magnetic pre-sheath entrance was assumed to bi-Maxwellian. The theoretical expression for the spatial extension of the pre-sheath it appears to be consistent with the simulations of Ref. 7. In Refs. 8 and 9, the structure of the system (the magnetic pre-sheath + the Debye sheath) different from papers in Refs. 6 and 7 is investigated by means of non-stationary (time-dependent) kinetic equations for electrons and ions. The electrons are described by the kinetic equation parallel to the magnetic field and the ion VDF is characterized by three components of the velocity. At the pre-sheath entrance, both electron and ion VDFs are chosen as Maxwellian (for the ion VDF also the smoothing factor is used[6]). The time dependence allowed the authors to give spatial distributions in the sheath for all parameters (densities, the electric potential, the electric field, and currents) for different fixed time-moments. It is found that the electrons running along the magnetic field lines attempt to catch the gyrating ions. Below the critical angle of the magnetic field incidence, such electron-ion interaction can lead to the appearing of the low frequency oscillations. For angle larger than the critical one, however the usual classical results are recovered. In all papers,[6–9] the collisional sheath located beyond the magnetic pre-sheath is not considered.

The DS and MPS regions are separated by the "presheath edge," or "sheath entrance (SE)," which in the A3S limit is characterized by the "marginal Bohm criterion," $u_z = \sqrt{k(T_e + \gamma T_i)}$, where u_z is the z-component of the ion fluid velocity, k is the Boltzmann constant, γ is the local ion polytropic coefficient, T_e is the electron temperature, and T_i is the ion temperature.[10] In this limit, the presheath edge appears as a field singularity if viewed on the MPS scale, and as lying in infinity if viewed on the DS scale. The present paper shows that (i) *the MPS and the CPS are separated by a similar (so far unknown) boundary surface, called the "MPS entrance (MPSE);" (ii) quite in analogy with the DSE, the MPSE can be defined in the A3S limit as a surface were the electric field has a singularity if viewed on the CPS scale and lies in infinity if viewed on the MPS scale*; (iii) *the kinetic form of the "Bohm–Chodura condition" at the MPS entrance is for the first time formulated as a quite logical consequence of the above mentioned conditions; (iv) we analyze the MPS – CPS and DS – MPS transition (intermediate) regions in the A3S limit. The equations bridging these regions and their characteristic lengths are determined.*

According to the Bohm–Chodura condition, the ion flow velocity at the MPS entrance should be aligned along the magnetic field lines. Therefore, the dominant effect of the MPS is to deflect the ion orbits in such a way that the velocity component, perpendicular to the wall, at the DS entrance (DSE) can fulfill the Bohm condition.[1,11] In the absence of a magnetic field or in the presence of a magnetic field perpendicular to the wall, the MPS does not exist as a distinct region at all.

II. MODEL AND BASIC EQUATIONS

The problem considered is one-dimensional, with the z axis perpendicular to the wall surface. The latter is placed at $z = 0$ and the plasma occupies the region $z < 0$. We assume a uniform magnetic field lying in the xz–plane and making a small angle α with the wall (see Fig. 2). The wall has a negative potential and all particles impinging on it are absorbed. The plasma is weakly ionized and composed of singly charged ions, electrons, and a cold neutral gas background,

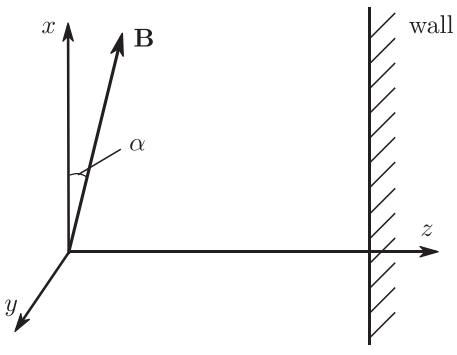

FIG. 2. MPWT geometry.

distributed uniformly. The thermal motion of ions is also neglected, $T_i \to 0$, whereas the electrons are the Boltzmann-distributed

$$n_e = n_0 \exp\left[e\Phi(z)/(kT_e)\right], \tag{1}$$

where $\Phi(z)$ is the electric potential.

The density distribution (1), which is most often used, may be incorrect especially near walls, where absorption of fast electrons tends to decrease the electron density, in comparison with (1). Some aspects of the validity of the Boltzmann relation (1) for electrons in the magnetized plasma is discussed in Ref. 12, although the conditions found in Ref. 12 hardly can be applied to our one-dimensional case. Our choice of the form (1) can be justified because the electrons, having high mobility and moving along the magnetic field lines, can achieve Boltzmann-like distribution due to collision processes (See Sec. III B below) and the reflection of electrons by the negative potential barrier at the wall.[2] The ions are assumed to be produced by the electron-neutral impact ionization accounted for by the source term proportional to the ionization frequency ν_i, and governed also by the charge-exchange collisions with the neutrals. For the ions' distribution function $f_i(z, \mathbf{v})$, we have the kinetic equation

$$v_z\frac{\partial f_i}{\partial z} - \frac{e}{m_i}\frac{\partial\Phi}{\partial z}\frac{\partial f_i}{\partial v_z} + (\mathbf{v}\times\mathbf{B})\frac{\partial f_i}{\partial \mathbf{v}} = \delta(\mathbf{v})\int d\mathbf{v}_n \nu_{cx}(|\mathbf{v}_n|) f_i(z,\mathbf{v}) - \nu_{cx}(|\mathbf{v}|) f_i + \nu_i\delta(\mathbf{v})\cdot n_e(z), \tag{2}$$

where Φ is the electric potential, $\mathbf{B} = \{B\cos\alpha, 0, B\sin\alpha\}$ is the magnetic field (Fig. 2); first two terms in the right-hand-side describe the charge-exchange collisions of ions with the cold neutrals with the frequency $\nu_{cx}(|\mathbf{v}|) = |\mathbf{v}|/\lambda_{cx}$. The gas of neutrals is homogeneous in space (their number density $n_n = \text{const}$) and follow the distribution function $f_n = n_n\delta(\mathbf{v})$. The contribution of the Dirac δ–function just from the latter expression is occurring in Eq. (2). In the MPWT theory, the model of the constant charge-exchange length, $\lambda_{cx} = \text{const}$, is considered as a good approximation.[13]

Further we use the dimensionless quantities

$$-e\Phi/(kT_e) = \varphi, \quad \rho_i = c_s/\omega_c, \quad c_s^3 f_i/n_0 = f, \quad n_i/n_0 = \lambda_i, \quad c_s = \sqrt{kT_e/m_i}, \quad \omega_c = eB/m_i. \tag{3}$$

For convenience, the normalized phase-space velocity and the normalized electron density we denote with the same symbols as the non-normalized ones

$$\mathbf{v}/c_s \Rightarrow \mathbf{v}, \quad n_e/n_0 \Rightarrow n_e = e^{-\varphi}. \tag{4}$$

Introducing the unit vector $\boldsymbol{\tau}$ along the magnetic field direction, we obtain $\mathbf{B} = B\boldsymbol{\tau}$. In Eqs. (3), ρ_i represents a characteristic gyro-radius of ions. In these quantities, the system of equations used below acquire the form

$$v_z\frac{\partial f_i}{\partial z} + \frac{\partial\varphi}{\partial z}\frac{\partial f_i}{\partial v_z} + \frac{1}{\rho_i}(\mathbf{v}\times\boldsymbol{\tau})\frac{\partial f_i}{\partial v} = \frac{1}{\lambda_{cx}}\left[\delta(\mathbf{v})C(z) - |\mathbf{v}|f_i\right] \tag{5}$$

with

$$C(z) = \int d\mathbf{v}|\mathbf{v}|f_i(z,\mathbf{v}) + \frac{\lambda_{cx}}{\lambda_i}e^{-\varphi}, \tag{6}$$

$$n = \int d\mathbf{v} f_i(z,\mathbf{v}), \tag{7}$$

$$\mathbf{j} = \int d\mathbf{v}\mathbf{v} f_i(z,\mathbf{v}), \tag{8}$$

$$\lambda_D^2\frac{\partial^2\varphi}{\partial z^2} = b - e^{-\varphi}, \quad \lambda_D = \sqrt{4\pi e^2/(kT_e)}. \tag{9}$$

Here, λ_{cx} represents the ion mean free path at their charge-exchange collisions with neutrals. Its connection with the characteristic scale-length ℓ of the CPS will be discussed below. Equations (6)–(9) represent the system of partial integro-differential equations. Using the inequalities $\lambda_D \ll \rho_i \ll \ell$ and splitting the MPWT layer into three—CPS, the MPS, and DS sub-layers, we have succeeded to describe analytically the shape of the electric potential for these sub-layers separately and then connect the profiles of the potentials of the neighbour sub-layers in the continuous manner.

III. REGION OF THE CPS SUB-LAYER

In this section, we will give the explanation on the *Ion distribution function*, the *Electron distribution function,* and the *Bohm–Chodura criterion*.

A. Ion distribution function

The CPS can be completely separated and investigated independently from other sub-layers under the condition $(\rho/\ell) \to 0$. In order to find the ion distribution function in this limit, we can apply the method usually used in simplifying the kinetic equation for describing the motion of the guiding centres.[14] As in Ref. 14, we write Eq. (5) in a cylindrical coordinate system in velocity space with the axis along the magnetic field

$$v_z\frac{\partial f_i}{\partial z} + \frac{1}{v_\perp}\frac{\partial}{\partial v_\perp}v_\perp a_\perp f_i + \frac{\partial}{\partial v_\parallel}a_\parallel f_i + \frac{1}{v_\perp}\frac{\partial}{\partial\theta}a_\theta f_i = \frac{1}{\lambda_{cx}}\left[\delta(\mathbf{v})C(z) - |\mathbf{v}|f_i\right]. \tag{10}$$

Here, $v_\parallel$ and $v_\perp$ are the velocity components parallel and perpendicular to the magnetic field, respectively. In these quantities, the characteristic equations are

$$\frac{dz}{dt} = v_z, \tag{11}$$

$$\boldsymbol{a} = \frac{d\mathbf{v}}{dt} = \dot{\mathbf{v}} = \left(v_z\cdot\frac{\partial}{\partial z}\right)\mathbf{v} = \nabla\varphi + \frac{1}{\rho_i}(\mathbf{v}\times\boldsymbol{\tau}). \tag{12}$$

The velocity we can represent in the form

$$\mathbf{v} = v_\parallel\boldsymbol{\tau} + \mathbf{v}_D + v_\perp(\boldsymbol{\tau}_1\sin\theta + \boldsymbol{\tau}_2\cos\theta). \tag{13}$$

The vectors $\boldsymbol{\tau}_1$ and $\boldsymbol{\tau}_2$ are unit vectors that form a right-handed orthogonal triad with $\boldsymbol{\tau}$. In Fig. 3, the definite

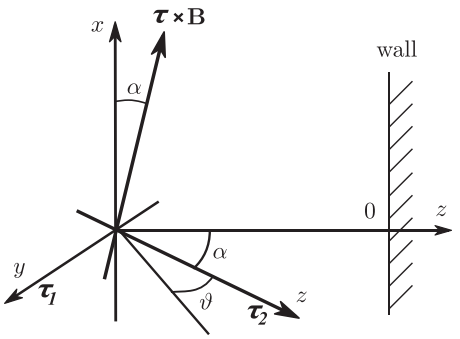

FIG. 3. Directions of the triad (τ, τ_1, τ_2).

directions of this triad are given, though the direction of these vectors are not important for the results in this section since they do not appear in the final result. The quantity $\mathbf{v}_D$ is the electric drift velocity of charged particles in crossed electric and magnetic fields

$$\mathbf{v}_D = \rho_i(\nabla\varphi \times \boldsymbol{\tau})\,. \tag{14}$$

Here and below $\nabla \equiv \{0, 0, \partial/\partial_z\}$. In the analysis of the particle motion in the crossing electric and magnetic fields,[14,15] the velocity $\mathbf{v}_D$ is conventionally separated out in accordance with Eq. (13). Substituting Eq. (13) into Eq. (12), we find

$$\begin{aligned}&\dot{v}_\parallel\boldsymbol{\tau} + \dot{\mathbf{v}}_D + \dot{v}_\perp\{\boldsymbol{\tau}_1\sin\theta + \boldsymbol{\tau}_2\cos\theta\}\\ &\quad + v_\perp\dot{\theta}\{\boldsymbol{\tau}_1\cos\theta - \boldsymbol{\tau}_2\sin\theta\}\\ &\quad = \boldsymbol{\tau}(\nabla\varphi\cdot\boldsymbol{\tau}) + \frac{1}{\rho_i}v_\perp\{\boldsymbol{\tau}_1\cos\theta - \boldsymbol{\tau}_2\sin\theta\}\,.\end{aligned} \tag{15}$$

Taking projections in the directions $\boldsymbol{\tau}_1$, $\{\boldsymbol{\tau}_1\sin\theta + \boldsymbol{\tau}_2\cos\theta\}$, and $\{\boldsymbol{\tau}_1\cos\theta + \boldsymbol{\tau}_2\sin\theta\}$, we find

$$a_\parallel = \dot{v}_\parallel = (\boldsymbol{\tau}\cdot\nabla\varphi)\,, \tag{16}$$

$$\begin{aligned}a_\perp = \dot{v}_\perp &= -\{(v_\perp\boldsymbol{\tau}\cdot\nabla)(\boldsymbol{\tau}_1\cdot\mathbf{v}_D)\cdot\sin\theta\\ &\quad + (v_\parallel\boldsymbol{\tau}\cdot\nabla)(\boldsymbol{\tau}_2\cdot\mathbf{v}_D)\cdot\cos\theta\}\\ &= A_1\sin\theta + B_1\cos\theta\,,\end{aligned} \tag{17}$$

$$a_\theta = v_\perp\cdot\theta = \frac{1}{\rho_i}v_\perp + \frac{v_\perp}{2}(\boldsymbol{\tau}\cdot\mathrm{curl}\mathbf{v}_D) + A_2\sin\theta + B_2\cos\theta\,. \tag{18}$$

In Eqs. (16)–(18), we have omitted the terms proportional to $\sin2\theta$ and $\cos2\theta$, and the relation $(\boldsymbol{\tau}\cdot\mathbf{v}_D) = 0$ taken into account. The coefficients A_1, B_1, A_2, B_2 do not contain the angle θ and their explicit forms are not important in the following analysis. Substituting $a_\parallel$ and $a_\perp$ into Eq. (10), the latter can be reduced to the form

$$\begin{aligned}&\left\{(v_\parallel\tau_z + v_{Dz})\frac{\partial}{\partial z} + \frac{\partial}{\partial v_\parallel}(\nabla\varphi\cdot\boldsymbol{\tau}) + \frac{1}{\rho_i}\frac{\partial}{\partial\theta}\right.\\ &\quad \left. + \frac{1}{2}(\boldsymbol{\tau}\cdot\mathrm{curl}\mathbf{v}_D)\frac{\partial}{\partial\theta} + A\sin\theta + B\cos\theta\right\}f_i\\ &\quad = \frac{1}{\lambda_{cx}}\left\{\delta(v_\perp\sin\theta + v_D)\delta(v_\perp\cos\theta)\delta(v_\parallel)C(z)\right.\\ &\quad \left. - \sqrt{v_\perp^2 + v_D^2 + v_\parallel^2 + 2v_\perp v_D\sin\theta}f_i\right\},\end{aligned} \tag{19}$$

where the coefficients A and B are again independent from the angle θ. If $(\rho_i/\ell) \ll 1$, the solution of Eq. (19) we can seek in the form of expansion in powers of (ρ_i/ℓ):

$$f_i = f_0 + \frac{\rho_i}{\ell}f_1 + \cdots\,. \tag{20}$$

In the zero approximation,

$$\frac{\partial f_0}{\partial\theta} = 0\,, \tag{21}$$

i.e., $f_0 = f_0(z, v_\parallel, v_\perp)$; Here, it should be mentioned that $v_D \approx \rho_i/\ell$. The function f_1 one can find from the equation

$$\begin{aligned}&\left\{(v_\parallel\tau_z + v_{Dz})\frac{\partial}{\partial z} + \frac{\partial}{\partial v_\parallel}(\nabla\varphi\cdot\boldsymbol{\tau}) + A\sin\theta + B\cos\theta\right\}f_0\\ &\quad = \frac{\partial f_1}{\partial\theta} + \frac{1}{\lambda_{cx}}\left\{\delta(v_\perp\sin\theta)\delta(v_\perp\cos\theta)\delta(v_\parallel)C(z)\right.\\ &\quad \left. - \sqrt{v_\perp^2 + v_\parallel^2}f_0\right\}.\end{aligned} \tag{22}$$

From physical consideration, we assume f_1 to be a periodic function of the angle θ. Obviously in our case, $v_{Dz} = 0$ and $\tau_z = \sin\alpha$. Consequently, the characteristic scale length ℓ should be chosen in the form $\ell = \lambda_{cx}\sin\alpha$, showing that the scale-length along the z-axis differs from the λ_{cx}. Introducing the normalized coordinate $x = (z/\ell)$ and integrating Eq. (22) over θ from 0 to 2π, we obtain an equation for ions in the CPS

$$v_\parallel\frac{\partial f_0}{\partial x} + \frac{\partial\varphi}{\partial x}\frac{\partial f_0}{\partial v_\parallel} + \sqrt{v_\perp^2 + v_\parallel^2}f_0 = \frac{\delta(v_\perp)\delta(v_\parallel)C(x)}{2\pi v_\perp}\,. \tag{23}$$

In obtaining Eq. (23), the relation $v_\parallel \gg v_D$ is taken into account. Obviously, due to the presence of the absorbing wall, the ions can move only in the positive direction towards the wall along the magnetic field line. The solution of Eq. (23) we will seek in the form

$$f_0 = \begin{cases}\dfrac{1}{2\pi v_\perp}\delta(v_\perp)f(x, v_\parallel), & v_\parallel \geq 0,\\ 0, & v_\parallel < 0\,.\end{cases} \tag{24}$$

For $f(x, v_\parallel)$, then we obtain the equation

$$v_\parallel\frac{\partial f}{\partial x} + \frac{\partial\varphi}{\partial x}\frac{\partial f}{\partial v_\parallel} = \delta(v_\parallel)C(x)\,, \tag{25}$$

with

$$C(x) = \int_0^\infty v_\parallel f(x, v_\parallel)dv_\parallel + \frac{\lambda_{cx}}{\lambda_i}e^{-\varphi}\,. \tag{26}$$

The solution of Eq. (25) with the boundary condition, $f = \delta(v_\parallel)$ at $\varphi = 0$, is

$$\begin{aligned}f(\varphi, y) = &\sqrt{2|y-\varphi|}\cdot\delta(\varphi - y)\cdot\exp\{-[x(\varphi) - x(0)]\}\\ &+ C(\varphi - y)x'(\varphi - y)\cdot\exp\{-[x(\varphi) - x(\varphi - y)]\}\\ &\times \mathrm{H}(\varphi - y)\mathrm{H}(y),\end{aligned} \tag{27}$$

where $x' \equiv dx(\varphi)/d\varphi$, $y = v_\parallel^2/2$, and H(y) is the Heaviside step function. By means of (7) and (27) for the expression of the ion density and the flux along the magnetic field-lines, we find

$$n(\varphi) = \int_0^\infty \frac{dy}{\sqrt{y}} \sqrt{|y-\varphi|}\delta(y-\varphi)\exp\left[x(\varphi)-x(0)\right] + \frac{1}{\sqrt{2}}\int_0^\varphi \frac{d\varphi'}{\sqrt{\varphi-\varphi'}} C(\varphi')x'(\varphi')\exp\left[x(\varphi')-x(\phi)\right], \quad (28)$$

$$j_\parallel(\varphi) = \int_0^\varphi d\varphi' C(\varphi')x'(\varphi')\exp[x(\varphi')-x(\phi)], \quad (29)$$

and for the coefficient $C(x)$ from (26), we obtain

$$C(\varphi) = j_\parallel(\varphi) + \frac{\lambda_{cx}}{\lambda_i} e^{-\varphi}. \quad (30)$$

In obtaining Eqs. (27) and (28), the monotonic dependence of the potential on the coordinate is also used, which means the one-to-one correspondence of the function $\varphi = \varphi(x)$ to its argument. From Eq. (30), we find

$$\frac{\partial j_\parallel}{\partial \varphi} = \left[C(\varphi) - j_\parallel(\varphi)\right]x'(\varphi) \quad \text{or} \quad j_\parallel(\varphi) = \frac{\lambda_{cx}}{\lambda_i}\int_0^\varphi d\varphi' e^{-\varphi'}x'(\varphi') \quad (31)$$

that allows to represent the coefficient $C(\varphi)$ in the form, more convenient for further consideration

$$C(\varphi) = \frac{\lambda_{cx}}{\lambda_i}\left\{\int_0^\varphi d\varphi' e^{-\varphi'}x'(\varphi') + e^{-\varphi}\right\}. \quad (32)$$

For the distribution function with $\varphi \neq 0$ from (24) and (27), we find

$$f_0(v_\perp, y, \varphi) = \frac{1}{2\pi v_\perp}\delta(v_\perp)C(\varphi-y)x'(\varphi-y) \times \exp\left\{-\left[x(\varphi)-x(\varphi-y)\right]\right\}\mathrm{H}(\varphi-y)\mathrm{H}(y). \quad (33)$$

B. Electron distribution function

In considering the electron kinetics, one has to take into account in principle the electron–electron, the electron–ion, and the electron–neutral particles collisions. In our case of the PWT layer with the prevailing density of neutrals, the main contribution is given by electron–neutral collisions. For not too high electron temperatures, the frequency of the inelastic electron–neutral collision is smaller in comparison with the elastic one and the influence of this type of collisions on the electron kinetics can be neglected. In order to find the electron distribution function, the kinetic equation of type (2) can be used with the electron–neutral elastic collision term on the right-hand side. This term can be represented in the form found by Kramers.[16]

One can further repeat word for word the whole procedure realized in Sec. III A for the ion distribution function. Using smallness of the parameter $(\rho_e/\ell_{en}) \ll 1$ (ρ_e is the electron gyro-radius and ℓ_{en} in the electron–neutral collations mean-free path) the electron distribution function we can represent in the form of the expansion (20) and reduce the corresponding kinetic equation to the form analogous to Eq. (25). As a solution of the latter for the electron distribution, we find

$$f_e = \text{const}\cdot\exp\left[-\frac{1}{T_e}\left(\frac{m_e v_\parallel^2}{2} + e\Phi(x)\right)\right], \quad (34)$$

which leads to the expression (1) for the electron density.

These results can be easily generalized for the case when together with electron–neutral collisions the electron–electron and the electron–ion collisions are also taken into account. The corresponding collision terms can be represented in the forms given in Ref. 17. It should be mentioned that the expression (34) for the electron distribution (and consequently the expression (1) for the electron density) is valid also for the MPS.

Due to the smallness of the Debye length ($\lambda_D \ll \ell_{en}$) in the DS, the collisions processes with the electrons participation can be neglected. The corresponding electron kinetic equation then becomes homogeneous (the right-hand side is equal to zero) and its solution, i.e., the electron distribution function, represents an arbitrary function of the total energy $f_e = f_e(m_e v^2/2 + e\Phi)$. From the boundary functions in the MPST–DS interface, it follows that this arbitrary function (i.e., the electron VDF) and the electron density can be expressed in forms (34) and (1), respectively.

C. Potential profile

Using the normalized coordinate x defined above, on the left-hand-side of the Poisson Eq. (9) appears a coefficient $(\lambda_D/\ell)^2$ and applying our assumption for the CPS, $(\lambda_D/\ell) \to 0$, Eq. (9) will be reduced to the condition of the quasineutrality,

$$n = e^{-\varphi}. \quad (35)$$

In terms of Eq. (28), this condition acquires the form of an equation for the electric potential φ:

$$\exp[-\varphi + x(\varphi)] = \int_0^\infty \frac{dy}{\sqrt{y}}\sqrt{|y-\varphi|}\delta(y-\varphi)\exp[x(0)] + \frac{1}{\sqrt{2}}\int_0^\varphi \frac{d\varphi}{\sqrt{\varphi-\varphi'}} C(\varphi')x'(\varphi')\exp[x(\varphi')]. \quad (36)$$

With the integral equation of the form

$$\int_0^\varphi \frac{d\varphi' S(\varphi')}{\sqrt{\varphi-\varphi'}} = g(\varphi), \quad (37)$$

we can manipulate as follows: from Eq. (37), we can write

$$\int_0^\varphi \frac{d\varphi'}{\sqrt{\varphi-\varphi'}}\int_0^{\varphi'} \frac{d\varphi''\Psi(\varphi'')}{\sqrt{\varphi'-\varphi''}} = \int_0^\varphi \frac{d\varphi' g(\varphi')}{\sqrt{\varphi-\varphi'}}; \quad (38)$$

changing the ordering of integrations by means of equality

$$\int_{\varphi''}^{\varphi} \frac{d\varphi'}{\sqrt{(\varphi-\varphi')(\varphi'-\varphi'')}} = \pi, \tag{39}$$

we find

$$\psi(\varphi) = \frac{1}{\pi}\frac{d}{d\varphi}\int_0^{\varphi} \frac{d\varphi' g(\varphi')}{\sqrt{\varphi-\varphi'}}\,. \tag{40}$$

Applying this manipulation to Eq. (36), we obtain

$$\int_0^{\varphi} \frac{d\varphi' \exp[-\varphi + x(\varphi)]}{\sqrt{\varphi-\varphi'}} = \frac{\pi}{\sqrt{2}}\int_0^{\varphi} \varphi'' C(\varphi'')\frac{d}{d\varphi''}\exp[x(\varphi'')]\,. \tag{41}$$

Using the relation (32), we represent the equation for finding the inverse to $\varphi = \varphi(x)$ function $x = x(\varphi)$ in the form

$$A\cdot e^{-\varphi}x'(\varphi) = \frac{\partial}{\partial\varphi}e^{-x(\varphi)}\int_0^{\varphi}\frac{d\varphi' \exp[-\varphi' + x(\varphi')]}{\sqrt{\varphi-\varphi'}}\,, \tag{42}$$

where $A = \frac{\pi}{\sqrt{2}}\frac{\lambda_{cx}}{\lambda_i}$. For $\varphi \ll 1$ from Eq. (42), we find

$$x(\varphi) = x(0) + \frac{2}{A}\sqrt{\varphi}\left\{1 - \frac{2}{A}\sqrt{\varphi}\left(1-\frac{\pi}{4}\right)\right\}. \tag{43}$$

From Eq. (42), it is obvious that at the point, $x = x_m$, where

$$\frac{\partial}{\partial\varphi}\int_0^{\varphi}\frac{d\varphi' \exp[-\varphi' + x(\varphi')]}{\sqrt{\varphi-\varphi'}} = 0\,, \tag{44}$$

the value $dx/d\varphi$ equals zero, which means that the electric field ($E \propto d\varphi/dx$) has a singularity, $E(x) \to\infty$ at $x \to x_m$. We define this point as the MPS entrance (MPSE) or as the edge of the CPS. This newly defined MPSE is quite analogous to the definition of the DS entrance in the unmagnetized PWT layer.[11] The potential profile resulting from Eq. (40) is shown in Fig. 4. The curve starts with zero field and really ends with a field singularity, $x'(\varphi) = 0$, at the MPS edge

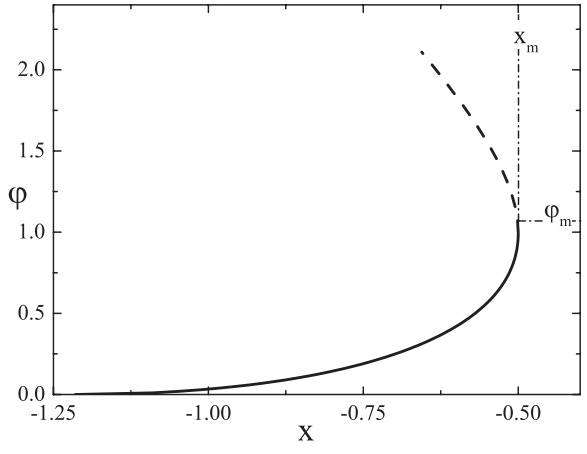

FIG. 4. The quasineutral potential profile $\varphi = \varphi(x)$ in the CPS. The parameter $A = 1.6$. The MPSE is indicated by the vertical line $x = x_m$, $\varphi \geq \varphi_m$.

($\varphi = \varphi_m$, $x = x_m$). The numerical calculations give for $x_m = 0.5$ and for $\varphi(x_m) = \varphi_m$. The parameter $A = 1.6$ that means $\lambda_{ck} \approx 0.72\lambda_i$. Close to the singular point, a parabolic dependence takes place

$$x = x_m - a(\varphi_m - \varphi)^2, \tag{45}$$

where $a \simeq 0.22$. The relation (45) is valid in rather large interval $0.75 \leq \varphi \leq 1.25$.

D. Bohm–Chodura criterion

According to Eq. (28), the expression for the ion density for $\varphi \neq 0$ we can represent in the form

$$n(\varphi) = \int_0^{\varphi}\frac{dy}{\sqrt{y}}\tilde{f}(\varphi - y)\exp[-x(\varphi)], \tag{46}$$

where

$$\tilde{f}(\varphi - y) = \frac{1}{\sqrt{2}}C(\varphi - y)x'(\varphi - y)\exp[x(\varphi - y)]. \tag{47}$$

Considering the density as a moment of the "zero order," $n(\varphi) = M_0(\varphi)$; for "$n$th order moment," we find

$$M_n(\varphi) = \int_0^{\varphi} d\varphi'(\varphi - \varphi')^{n-1/2}\tilde{f}(\varphi')\exp[-x(\varphi)]. \tag{48}$$

From Eq. (47) at $n \neq 1/2$, it follows the recurrence relation

$$\frac{d}{d\varphi}M_n(\varphi) = \left(n - \frac{1}{2}\right)\int_0^{\varphi} d\varphi'(\varphi - \varphi')^{n-1-1/2} \times \tilde{f}(\varphi')\exp[-x(\varphi)] - x'(\varphi)M_n(\varphi)\,. \tag{49}$$

At the MPS edge, $n(\varphi_m) = \exp(\varphi_m)$ and consequently $M_0(\varphi_m) = \exp(\varphi_m)$. Then according to Eq. (49) and the condition $x'(\varphi_m) = 0$,

$$M_{-1}(\varphi_m) = 2\exp(\varphi_m)\,, \tag{50}$$

and finally we find

$$\frac{1}{n(\varphi_m)}\int_0^{\varphi_m}\frac{dy}{y^{2/3}}\tilde{f}(\varphi_m - y)\exp[-x(\varphi_m)] = 2\,. \tag{51}$$

It means that the kinetic Bohm–Chodura criterion is fulfilled in the marginal form.[18] In the integral (48), do not arise mathematical difficulties due to divergence at the point $y = 0$ in the denominator of the integrand, as at this point the distribution function vanishes [see Eq. (47)].

IV. REGION OF THE MPS

As it is mentioned above, the MPS region is assumed to be collisionless, as its characteristic scale-length is much smaller than the characteristic mean-free-path, $\rho_i \ll \lambda_{cx}$. The neglecting of the right-hand side in Eq. (5) becomes obvious if we introduce the new coordinate variable $\eta = z/\rho_i$. To simplify the use of the boundary condition at $\varphi = \varphi_m$ and

matching of the solutions, it is convenient to turn the coordinate system on angle α choosing the polar axis along the magnetic field direction [$\tilde{f}(\varphi_m) = 0$, see Fig. 3]. For the velocity components in the new system, we find

$$\begin{aligned} u_x &= v_x \cos\alpha + v_y \sin\alpha\,, \\ u_y &= v_y\,, \\ u_z &= -v_x \sin\alpha + v_z \cos\alpha\,. \end{aligned} \tag{52}$$

By means of relations (52) at the small inclination angle $\alpha(\ll 1)$, Eq. (5) acquires the form

$$\begin{aligned} u_z \frac{\partial \bar{f}_i}{\partial \eta} + u_z \frac{\partial \bar{f}_i}{\partial u_y} + \left\{ \frac{\partial \varphi}{\partial \eta} - u_y \right\} \frac{\partial \bar{f}_i}{\partial u_z} \\ = -\alpha \left\{ u_x \frac{\partial \bar{f}_i}{\partial \eta} + \frac{\partial \varphi}{\partial \eta} \frac{\partial \bar{f}_i}{\partial u_x} \right\}. \end{aligned} \tag{53}$$

The solution of Eq. (53) will be sought in the form

$$\bar{f}_i = \bar{f}_0 + \alpha \bar{f}_1\,. \tag{54}$$

Then from (53), we have

$$u_z \frac{\partial \bar{f}_0}{\partial \eta} + u_z \frac{\partial \bar{f}_0}{\partial u_y} + \left\{ \frac{\partial \varphi}{\partial \eta} - u_y \right\} \frac{\partial \bar{f}_0}{\partial u_z} = 0\,, \tag{55}$$

$$\begin{aligned} u_z \frac{\partial \bar{f}_1}{\partial \eta} + u_z \frac{\partial \bar{f}_1}{\partial u_y} + \left\{ \frac{\partial \varphi}{\partial \eta} - u_y \right\} \frac{\partial \bar{f}_1}{\partial u_z} \\ = -\left\{ u_x \frac{\partial \bar{f}_0}{\partial \eta} + \frac{\partial \varphi}{\partial \eta} \frac{\partial \bar{f}_0}{\partial u_x} \right\}. \end{aligned} \tag{56}$$

The integration of Eq. (55) along the characteristics gives

$$\bar{f}_0 = \bar{f}_0\{u_x, u_y - \eta, u_z^2 + u_y^2 - 2\varphi(\eta) - (u_y - \eta)^2\}. \tag{57}$$

The solution of Eq. (56) also depends on u_z, therefore we have to distinguish the solutions with positive $(u_z > 0)\bar{f}_1^+$ and negative $(u_z < 0)\bar{f}_1^-$ velocities.

We expect (and following calculations confirm) that

(i) the width of the MPS sub-layer is of the order of ρ_i; This is quite commonly accepted assumption.[4,5,19,20] Below we show that in fact moving towards the MPS edge, the ions cover the distance $\lesssim \rho_i$.

(ii) Under our conditions, $\lambda_S \ll \rho_i \ll \lambda_{cx}$ the edge of the MPS sub-layer (or the DS's entrance), we define as a point, where the electric field, directed towards the wall, runs into singularity, $E_z \to \infty$, [See Refs. 11 and 20];

(iii) The ions under action of the electric field cannot outline the full Larmor-circle and at the DS entrance the ion velocities are directed along the z-axis. So in the MPS sub-layer ions, described by $\bar{f}_1^+$, move in the z-axis positive direction and $\bar{f}_0^- = 0$.

(iv) At the DS entrance, the Bohm criterion should be fulfilled.[1,11,20]

(v) Close to the MPS edge ions move along the z-axis and there In order to satisfy the Lenz law for the positively charged particles, rotating around the magnetic field line, in our right-handed coordinate system (see Fig. 3), the interval of the possible values for u_y should be chosen as follows: $-\infty \le \le 0$. [See Ref. 21].

All abovementioned items are in accordance with the ion trajectories' analysis given in Ref. 19. Below we will show that under the conditions (i)–(v), the electric potential φ_s at the MPS edge point, satisfies the relation

$$\varphi_s > (\omega_c \rho_i / c_s)^2 \simeq 1\,, \tag{58}$$

[see Eq. (72) and Table I].

In Ref. 19, the trajectories of ions in a MPS with a strongly tilted magnetic field are analyzed and found that if the ion gas is cold, $T_e > T_i$ at the fulfillment of the condition (58), in all probability they enter the DS sub-layer with considerable normal to the wall velocities ($u_y = 0$) and without oscillations along the z-axis (see discussions on the "type 2" trajectories in Sec. II D of Ref. 19 [on the ion distribution function with negative velocity, $u_z < 0$, at the cold ion source (neutrals) [see also Appendix].

Introducing the new variable $\bar{y} = u_z^2/2$, Eq. (56) can be represented in the form

$$\begin{aligned} u_z \frac{\partial \bar{f}_1^+}{\partial \eta} + u_z \frac{\partial \bar{f}_1^+}{\partial u_y} + \left\{ \frac{\partial \varphi}{\partial \eta} - u_y \right\} \frac{\partial \bar{f}_1^+}{\partial \bar{y}} \\ = -\frac{1}{\sqrt{2\bar{y}}} \left\{ u_x \frac{\partial \bar{f}_0}{\partial \eta} + \frac{\partial \varphi}{\partial \eta} \frac{\partial \bar{f}_0}{\partial u_x} \right\} \mathrm{H}(\bar{y})\,. \end{aligned} \tag{59}$$

Further, we integrate Eq. (59) along the characteristics and apply the boundary condition at the MPS entrance, defined by $\varphi = \varphi_m$,

$$\bar{f}_i|_{\varphi_m} = \{\bar{f}_0 + \alpha \bar{f}_1^+\}_{\varphi_m} = \bar{f}_0|_{\varphi_m}\,, \tag{60}$$

where the function $\bar{f}_0|_{\varphi_m}$ in the right-hand side is defined by the expression (33) at $\varphi - \varphi_m$. In the variables (u_x, u_y, u_z) from (52), this expression can be represented in the form

$$\bar{f}_0|_{\varphi_m} = \frac{1}{\pi} \delta\left(u_z^2 + u_y^2\right) S(u_x, \varphi_m)\,, \tag{61}$$

$$\begin{aligned} S(u_x, \varphi_m) = \int_0^{\varphi_m} x'(\overline{\varphi}) C(\overline{\varphi}) \exp[-x_m + x(\overline{\varphi})] \\ \times \delta\left[\varphi_m - \frac{1}{2}u_x^2 - \overline{\varphi}\right] d\overline{\varphi}\,, \end{aligned} \tag{62}$$

where $C(\overline{\varphi})$ is defined by Eq. (32). By means of Eqs. (53), (56), (61), (62) and boundary condition (60), we find the ion distribution function in the MPS sub-region

TABLE I. Coefficient A, potential φ_m at the CPS edge and parameter $I(\varphi_m)$.

A	0.16	0.4	1	1.6	2	2.2	3.4	4
φ_m	1.41	1.21	1.05	1	0.97	0.96	0.94	0.92
$I(\varphi_m)$	0.302	0.365	0.417	0.438	0.446	0.449	0.458	0.464

$$\bar{f}_i = \frac{1}{\pi}\delta\left[u_z^2+u_y^2-2(\varphi-\varphi_m)\right]S(u_x,\varphi_m)-\alpha \times \int_{\varphi_m}^{\varphi} \frac{\mathrm{H}\left\{u_z^2+u_y^2-2(\varphi'-\varphi_m)-\left(u_y-\left[\eta(\varphi)-\eta(\varphi')\right]\right)^2\right\}}{\sqrt{u_z^2+u_y^2-2(\varphi'-\varphi_m)-\left(u_y-\left[\eta(\varphi)-\eta(\varphi')\right]\right)^2}} \times d\varphi'\left\{u_x S(u_x,\varphi_m)\frac{\partial}{\partial\varphi}+\frac{\partial S(u_x,\varphi_m)}{\partial U_x}\right\} \times \frac{1}{\pi}\delta\left[u_z^2+u_y^2-2(\varphi-\varphi_m)\right]\mathrm{H}(u_z+\varepsilon_1)\mathrm{H}(-u_y+\varepsilon_2). \quad (63)$$

In Eq. (63), the infinitesimal values, $\varepsilon_1 \to +0$ and $\varepsilon_2 \to +0$, are introduced in order to satisfy Eq. (59) when u_z and u_y change in the intervals $0 \le u_z < \infty$ and $-\infty < u_y \le 0$.

A. Potential profile

By means of Eq. (63), we can calculate the ion density by integration over velocities **u**. The MPS sub-layer is quasi-neutral and using Eq. (35) we can construct an equation for the electric potential $\varphi \neq 0$, as it was made in Sec. III. In this section and below the coordinates, obtained under the quasineutrality condition,

$$e^{-\varphi} = \int d\mathbf{u}\cdot\bar{f}_i(\varphi,\mathbf{u};\overline{\eta}), \quad (64)$$

we will mark with bar-sign. According to the relation (36), the integration of the first term in the right-hand side of Eq. (63) over the velocities gives $\exp(-\varphi_m)$. Substituting the expression for the ion density into Eq. (35) and keeping in mind the smallness of α (that leads to the smallness of the difference $\varphi-\varphi'$), we find

$$B\left\{2(\varphi-\varphi_m)\right\}^{3/2} = F(\overline{A}), \quad B = \frac{\pi\exp(-\varphi_m)}{\alpha I(\varphi_m)}, \quad (65)$$

$$F(\overline{A}) = \int_{\overline{A}}^{1}\frac{dt}{\sqrt{1-t^2}}\frac{1-t(t-\overline{A})}{\sqrt{1-(t-\overline{A})^2}}, \quad (66)$$

$$\overline{A} = \frac{\overline{\eta}(\varphi)-\overline{\eta}(\varphi_m)}{\sqrt{2(\varphi-\varphi_m)}}, \quad (67)$$

where $\overline{A}$ changes in the interval $\overline{A}_s \le \overline{A} \le 1$, $(\varphi \ge \varphi_m)$. In obtaining of Eq. (65) the relations

$$\int_0^{\infty} du_x \frac{\partial S(u_x,\varphi_m)}{\partial u_x} = 0 \quad \text{and} \quad (68)$$

$$I(\varphi_m) = \int_0^{\infty} u_x S(u_x,\varphi_m)du_x = \frac{\lambda_{cx}}{\lambda_i}\int_0^{\varphi_m} e^{-\varphi'}x'(\varphi')d\varphi', \quad (69)$$

are used. The validity of the second equality in Eq. (68) can be proved by the relation

$$\int_0^{\varphi_m} x'(\varphi')C(\varphi')\exp[-x_m+x(\varphi')]d\varphi' = \frac{\lambda_{cx}}{\lambda_i}\int_0^{\varphi_m} e^{-\varphi'}x'(\varphi')d\varphi', \quad (70)$$

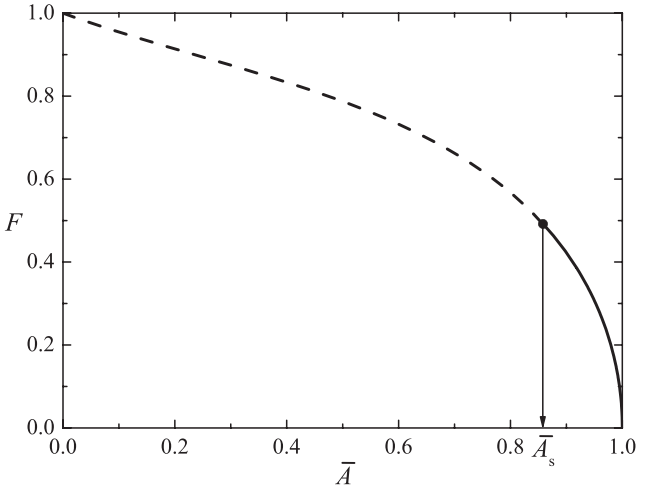

FIG. 5. Profile of the function $F(\overline{A})$. Solid line is the MPS region of interest, where $\overline{A}_s \le \overline{A} \le 1$.

which follows from the comparison of Eqs. (41) and (42). The function $F(\overline{A})$ decreases, when $\overline{A}$ grows, $F(\overline{A}) \to 0$ and $\partial F(\overline{A})/\partial\overline{A} \to -\infty$ at $\overline{A} \to 1$ (see Fig. 5). Taking derivative of Eq. (64) with φ, we find that $(\partial z/\partial\varphi) = 0$ at the point $\overline{A}_s$, where the following equality is fulfilled

$$3F(\overline{A}_s) = -\overline{A}_s\left.\frac{\partial F(\overline{A})}{\partial\overline{A}}\right|_{\overline{A}_s}. \quad (71)$$

Numerical calculations using the curve of Fig. 5 gives $\overline{A}_s = 0.873854$ and $F(\overline{A}_s) = 0.468221$. The potential profile in the MPS is given in Fig. 6. The point $z = z_s$ or $\varphi = \varphi_s$, where the electric field runs into singularity, we can considered as the MPS's edge or as the DS's entrance. The values of $\overline{A}_s$ and $F(\overline{A}_s)$ allow us to find from Eqs. (65) and (67)

$$\varphi_s-\varphi_m = \frac{1}{2}\left\{\frac{\alpha}{\pi}e^{\varphi_m}I(\varphi_m)F(\overline{A}_s)\right\}^{2/3}, \quad (72)$$

$$\text{and} \quad \overline{\eta}_s-\overline{\eta}_m = \overline{A}_s\left\{\frac{\alpha}{\pi}e^{\varphi_m}I(\varphi_m)F(\overline{A}_s)\right\}^{1/3}. \quad (73)$$

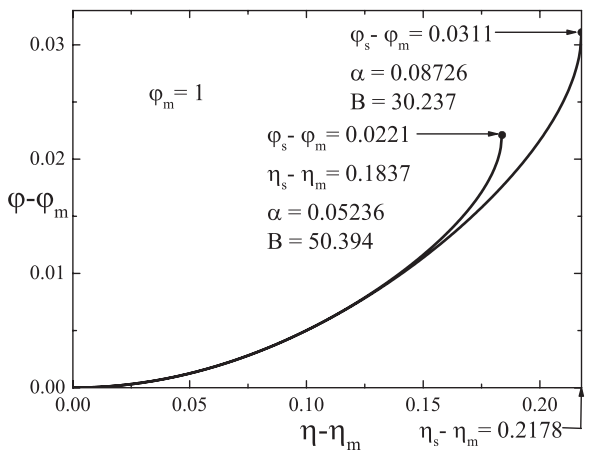

FIG. 6. Potential profiles in the MPS for $\alpha = 3°$ and $\alpha = 5°$.

1. Potential profile close to the MPS edge

Expanding the right-hand side of the relation (65) in the series near the point $\overline{A}_s$, we obtain

$$B\left[2(\varphi-\varphi_m)\right]^{3/2}=F(\overline{A}_s)+(\overline{A}-\overline{A}_s)\frac{\partial F(\overline{A})}{\partial\overline{A}}\Big|_{\overline{A}_s}+\cdots. \quad (74)$$

Using Eqs. (67) and (71)–(73), we find

$$\overline{\eta}=\overline{\eta}_s-b(\varphi-\varphi_s)^2, \quad (75)$$

$$b=2\overline{A}_s\left\{\frac{\alpha}{\pi}e^{\varphi_m}I(\varphi_m)F(\overline{A}_s)\right\}^{-2/3}. \quad (76)$$

Equation (75) correctly describes the electric field singularity at $\overline{z}=\overline{z}_s$.

2. Potential profile at the MPS entrance from the MPS side

Expanding the auxiliary function $F(\overline{A})$ from (65) in series of powers $(1-\overline{A})$ in the first un-vanishing approximation, we find $F(\overline{A})=\overline{A}\sqrt{1-\overline{A}^2}$. By means of (67), we obtain

$$\varphi-\varphi_m=\frac{1}{2}\left[\overline{\eta}(\varphi)-\overline{\eta}(\varphi_m)\right]^2+O\left[(\varphi-\varphi_m)^4\right]. \quad (77)$$

Hence, at $\overline{z}(\varphi)\to\overline{z}(\varphi_m)$, the electric field vanishes.

B. Matching of potential profiles in the CPS and the MPS regions

Comparison of expressions (45) and (77) shows that for connection of the potential shapes from both sides of the MPS and the CPS interface, we can as usually[11,20] introduce a characteristic scale-length $\overline{l}_m$ and the renormalized variables

$$z(\varphi)-z(\varphi_m)=l_m\zeta, \quad \varphi-\varphi_m=\beta W. \quad (78)$$

Obviously, the equation for the potential in the intermediate region, which bridges the CPS and the MPS subregions, must consistently describe both representations. By means of new variables from Eq. (78), this intermediate equation can read

$$2\frac{\rho_i^2}{l_m^2}\beta W^3=\zeta^2\left(W^2+\frac{l_m}{al\beta^2}\zeta\right). \quad (79)$$

Really if $l_m=\ell$ the left-hand side of Eq. (79) is negligibly small and we obtain $a\beta^2W_{\rm CPS}^2=-\zeta$, which corresponds to the potential shape (45); and if $l_m=\rho_i$, then we obtain the potential shape (77) in the form $2\beta W_{MPS}=\zeta^2$. Choosing

$$l_m=\rho_i\left(\frac{4}{a}\frac{\rho_i}{\ell}\right)^{1/3} \quad \text{and} \quad \beta=\frac{1}{2}\left(\frac{4}{a}\frac{\rho_i}{\ell}\right)^{2/3} \quad (80)$$

for the potential dependence in the vicinity of the CPS edge, we obtain

$$W^3=\zeta^2(W^2+\zeta). \quad (81)$$

The curve in Fig. 7 describes this dependence. The length l_m can be considered as a characteristic intermediate scale.

C. Bohm condition

Intending to connect later on the distribution functions in the MPS and the DS, it is convenient to represent the distribution function (63) in terms of the velocity components $[v_x, v_y, v_z$; see Eqs. (52)]:

$$\begin{aligned}\overline{f}_i(\varphi,v_x,v_y,v_z)&=\overline{f}_{0m}+\overline{f}_{1m}\\&=\frac{1}{\pi}\delta\left[v_z^2+v_y^2-2(\varphi-\varphi_m)\right]S(v_x,\varphi_m)-\frac{\alpha}{\pi}\int_{\varphi_m}^{\varphi}\frac{\partial\eta(\varphi')}{\partial\varphi'}\\&\times\frac{\mathrm{H}\left\{v_z^2+v_y^2-2(\varphi'-\varphi_m)-\left(v_y-\left[\eta(\varphi)-\eta(\varphi')\right]\right)^2\right\}}{\sqrt{v_z^2+v_y^2-2(\varphi'-\varphi_m)-\left(v_y-\left[\eta(\varphi)-\eta(\varphi')\right]\right)^2}}\\&\times\left\{v_y-\left[\eta(\varphi)-\eta(\varphi')\right]\right\}d\varphi'\\&\times\left\{v_xS(v_x,\varphi_m)\frac{\partial}{\partial\varphi}+\frac{\partial S(u_x,\varphi_m)}{\partial v_x}\right\}\\&\times\delta\left[v_z^2+v_y^2-2(\varphi-\varphi_m)\right]\mathrm{H}(v_z+\varepsilon_1)\mathrm{H}(-v_y+\varepsilon_2). \quad (82)\end{aligned}$$

Then for ion density and the presheath approximation (64), we have, respectively,

$$n(\varphi)=\int d\mathbf{v}\cdot\overline{f}_i(\varphi,v_x,v_y,v_z;\eta), \quad (83)$$

$$e^{-\varphi}=\int d\mathbf{v}\cdot\overline{f}_i(\varphi,v_x,v_y,v_z;\eta). \quad (84)$$

In fact Eq. (82) is the solution of Eq. (53) written in terms of velocity components v_x, v_y, v_z, and quite identical to the solution (63) with the accuracy of the first order of the coefficient α. Keeping in mind the one-to-one mutual dependence between φ and z, we can represent this equation in the form

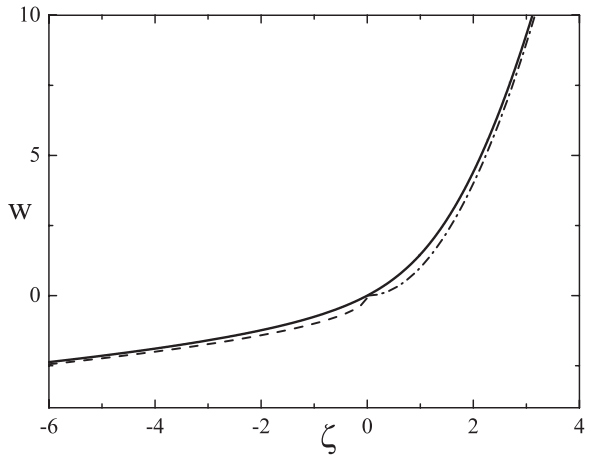

FIG. 7. The potential shape (solid line) in the CPS–MPS intermediate region with the CPS entrance $W_{\rm CPS}=-\sqrt{-\zeta}$ (dashed line) and the MPS entrance $W_{\rm MPS}=\zeta^2$ (dashed-dotted line).

$$\frac{\partial \overline{f}_i}{\partial \varphi}+\frac{1}{v_z}\frac{\partial \overline{f}_i}{\partial v_z} = \frac{1}{v_z}\frac{\partial z(\varphi)}{\partial \varphi}\frac{1}{\rho_i}\left\{v_y\left(\frac{\partial \overline{f}_i}{\partial v_z}-\alpha\frac{\partial \overline{f}_i}{\partial v_y}\right)-(v_z-\alpha v_x)\frac{\partial \overline{f}_i}{\partial v_y}\right\}. \quad (85)$$

Considering this relation at the MPS edge, where $(\partial z(\varphi)/\partial\varphi)=0$, after integration over velocities, we find

$$\left.\frac{(\partial n)\varphi}{\partial \varphi}\right|_{\varphi_s} = -\int_0^\infty dv_x\int_{-\infty}^0 dv_y\int_0^\infty dv_z \times\frac{1}{v_z}\frac{\partial}{\partial v_z}\overline{f}_{1m}(\varphi_s,v_x,v_y,v_z). \quad (86)$$

In obtaining Eq. (86), we have taken into account that the function $\overline{f}_{0m}$ from Eq. (82) does not give the contribution in the right-hand side of Eq. (86). For the ion density at the MPS edge, we have

$$n(\varphi_s)=\int d\mathbf{v}\{\overline{f}_{0m}+\overline{f}_{1m}\}=e^{-\varphi_m}-\int_0^\infty dv_x\int_{-\infty}^0 dv_y \times\int_0^\infty dv_z\overline{f}_{1m}(\varphi_s,v_x,v_y,v_z). \quad (87)$$

Using the quasineutrality relation $n_s=n(\varphi)=\exp(-\varphi_s)$ [see Eq. (64)] and condition $\overline{f}_{1m}(\varphi_s,v_x,v_y,v_z)=0$ at $v_z=0$, we find

$$\frac{1}{n_s}\int_0^\infty dv_z\frac{1}{v_z}\frac{\partial}{\partial v_z}\langle\overline{f}_{1m}(\varphi_s,v_z)\rangle=1, \quad (88)$$

$$\langle\overline{f}_{1m}(\varphi_s,v_z)\rangle=\int_0^\infty dv_x\int_{-\infty}^0 dv_y\overline{f}_{1m}(\varphi_s,v_x,v_y,v_z). \quad (89)$$

Hence at the MPS edge, the Bohm criterion is fulfilled also in the marginal form [cf. with Eq. (51)]. By means of the explicit expression of the distribution function $\overline{f}_{1m}$ from Eq. (82), the criterion (88) acquires the form

$$\frac{1}{n_s}\frac{\alpha}{8\pi}\frac{I(\varphi_m)}{(\varphi_s-\varphi_m)^{3/2}}\int_{\varphi_m}^{\varphi_s}d\varphi'\frac{d\eta(\varphi')}{d\varphi'}\frac{1}{\sqrt{\varphi'-\varphi_m}}=1. \quad (90)$$

V. DEBYE SHEATH

Traveling from the unperturbed plasma to the wall, the ions are first accelerated along the magnetic field lines in the photon correlation spectroscopy (PCS). In the MPS, they are reoriented towards the wall; and finally in the DS, they should strongly accelerated in the direction normal to the wall. The gradually increase of the potential in the MPS ends with the formal field singularity at $\varphi=\varphi_s$, representing the MPS edge. The quasineutral MPS cannot account for the boundary condition at the wall. It must be supplemented by the DS with characteristic scale-length λ_D, where the space charge becomes important. To resolve the shape of the potential in the thin DS, it is convenient to use appropriate space variable $\xi=z/\lambda_D$. On this scale, the MPS edge is infinitely remote. Therefore, we have the boundary condition $\varphi\to\varphi_s$ for $\xi\to-\infty$ (or equivalently $\partial\varphi/\partial\xi$ for $\varphi\to\varphi_s$).

According to the relation $\varepsilon_{Dm}=(\lambda_D/\rho_i)\to 0$ from Eq. (85), it follows that the ion distribution function in the DS f_{sh} must depend on the combination $(v_z^2/2)-\varphi$. Hence, like as it was made in Sec. IV [see Eq. (60)], there is no self-consistent kinetic problem, but the ion distribution function in the sheath should be explicitly determined from the MPS distribution (82) at the sheath edge

$$f_{sh}(v_z^2/2-\varphi_s)=\overline{f}_i(\varphi_s,v_x,v_y,v_z). \quad (91)$$

As a result, we find

$$\begin{aligned}\overline{f}_{sh}&=\overline{f}_{0m}+\overline{f}_{1m}\\&=\frac{1}{\pi}\delta\left[v_z^2+v_y^2-2(\varphi-\varphi_m)\right]S(v_x,\varphi_m)-\frac{\alpha}{\pi}\int_{\varphi_m}^{\varphi}\frac{\partial\eta(\varphi')}{\partial\varphi'}\\&\times\frac{\mathrm{H}\left\{v_z^2+v_y^2-2(\varphi'-\varphi_m)-\left(v_y-\left[\eta(\varphi)-\eta(\varphi')\right]\right)^2\right\}}{\sqrt{v_z^2+v_y^2-2(\varphi'-\varphi_m)-\left(v_y-\left[\eta(\varphi)-\eta(\varphi')\right]\right)^2}}\\&\times\left\{v_y-\left[\eta(\varphi)-\eta(\varphi')\right]\right\}d\varphi'\\&\times\left\{v_xS(v_x,\varphi_m)\frac{\partial}{\partial\varphi}+\frac{\partial S(u_x,\varphi_m)}{\partial v_x}\right\}\\&\times\delta\left[v_z^2+v_y^2-2(\varphi-\varphi_m)\right]\mathrm{H}(v_z+\varepsilon_1)\mathrm{H}(-v_y+\varepsilon_2). \quad (92)\end{aligned}$$

According to relations (72) and (73), the product of their left-hand sides is of the order of α, $(\varphi_s-\varphi_m)(\overline{\eta}_s-(\overline{\eta}_m)\propto\alpha$. Neglecting terms of the order of α^2, we can simplify the expression (92) and obtain

$$\begin{aligned}\overline{f}_{sh}&\simeq\frac{1}{\pi}\delta\left[v_z^2+v_y^2-2(\varphi-\varphi_m)\right]S(v_x,\varphi_m)\\&-\frac{\alpha}{\pi}\int_{\varphi_m}^{\varphi}\frac{\partial\eta(\varphi')}{\partial\varphi'}\frac{v_y\mathrm{H}\{v_z^2-2(\varphi'-\varphi_m)\}}{\sqrt{v_z^2-2(\varphi'-\varphi_m)}}d\varphi'\\&\times\left\{v_xS(v_x,\varphi_m)\frac{\partial}{\partial\varphi}+\frac{\partial S(u_x,\varphi_m)}{\partial v_x}\right\}\\&\times\delta\left[v_z^2+v_y^2-2(\varphi-\varphi_m)\right]\mathrm{H}(v_z+\varepsilon_1)\mathrm{H}(-v_y+\varepsilon_2). \quad (93)\end{aligned}$$

Carrying out the integration over velocity for the ion density, we find

$$n(\varphi)=e^{-\varphi_m}+\frac{\alpha}{4\pi}\frac{I(\varphi_m)}{\sqrt{\varphi-\varphi_m}}\int_{\varphi_m}^{\varphi_s}\frac{\partial\eta(\varphi')}{\partial\varphi'}\frac{d\varphi'}{\sqrt{\varphi-\varphi'}}. \quad (94)$$

Here, $\varphi\geq\varphi_s$; and at $\varphi=\varphi_s$, the right-hand side of Eq. (94) equals to the electron density at this point $n(\varphi_s)=\exp(-\varphi_s)$ [cf. with Eq. (87)]. The quantity $I(\varphi_m)$ is defined by Eq. (69).

A. Potential profile in the DS

Introducing new space variable ξ into Poisson's equation (9) yields

$$\frac{\partial^2\varphi}{\partial\xi^2} = n(\varphi) - e^{-\varphi}. \tag{95}$$

Here, in n, the expression (94) is implied. Using the boundary condition $\partial\varphi/\partial\xi \to 0$ for $\varphi \to \varphi_s$, after integration of Eq. (95), we get

$$\frac{1}{2}\left(\frac{\partial\varphi}{\partial\xi}\right)^2 = R(\varphi)\,, \tag{96}$$

$$R(\varphi) = e^{-\varphi_m}(\varphi - \varphi_s) + \frac{\alpha}{2\pi} I(\varphi_m) \int_{\varphi_m}^{\varphi_s} d\varphi' \frac{\partial\eta(\varphi')}{\partial\varphi'} \ln\left\{\frac{\sqrt{\varphi-\varphi_m}+\sqrt{\varphi-\varphi'}}{\sqrt{\varphi_s-\varphi_m}+\sqrt{\varphi_s-\varphi'}}\right\}. \tag{97}$$

This equation can be again integrated to yield the potential distribution in the form $\xi = \xi(\varphi)$. Using the wall boundary condition $\varphi = \varphi_w$ at $\xi = \xi(w)$ Eq. (96), we present in the form convenient for the numerical calculations

$$\xi - \xi_w = \int_{\varphi_w}^{\varphi} \frac{d\varphi'}{\sqrt{2R(\varphi')}}\,. \tag{98}$$

The resulting sheath potential profile related to the wall potential $\varphi_w = 5.4$ (floating potential in Argon) is shown in Fig. 8. To analyze the DS entrance vicinity, we expand $R(\varphi)$ in the series in powers of $(\varphi - \varphi_s)$. Restricting ourselves with the third power, from Eq. (96), we obtain

$$\xi = \xi_0 - 2\sqrt{\frac{3}{\left(\partial^3 R(\varphi)/\partial\varphi^3\right)_{\varphi_s}}} \cdot (\varphi - \varphi_s)^{-1/2} \tag{99}$$

and the Poisson's Eq. (95) in this approximation acquires the form

$$\frac{\partial^2\varphi}{\partial\xi^2} = \frac{1}{2}\left[\frac{\partial^3 R(\varphi)}{\partial\varphi^3}\right]_{\varphi_s} (\varphi - \varphi_s)^2. \tag{100}$$

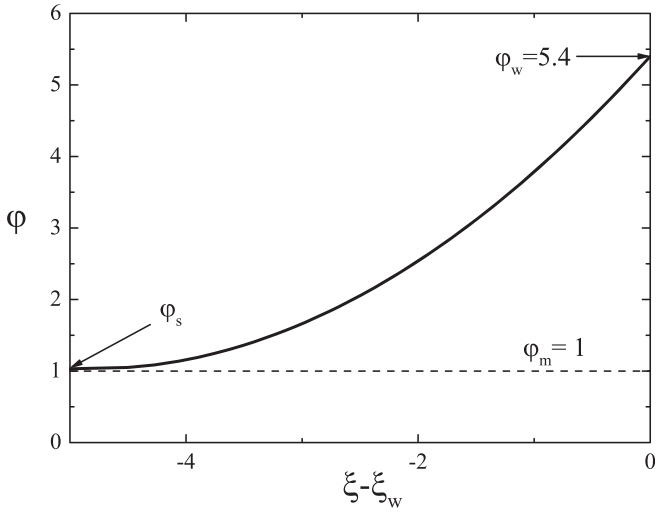

FIG. 8. Potential variation in the Debye sheath. The curves for $\alpha = 0.08727$ and $\alpha = 0.05236$ coincide.

The integration constant ξ_0 can be found by comparison of the dependence (98) with numerical curve given in Fig. 8. In obtaining (99) and (100), we have taken into account that in the expansion of $R(\varphi)$, the coefficient in front of the first power $(\varphi - \varphi_s)$ is zero due to quasineutrality condition at $\varphi = \varphi_s$ expressed by Eq. (94). The coefficient at $(\varphi - \varphi_s)^2$ also vanishes on account of the relation (88) [or Eq. (90)], representing the Bohm criterion.

B. Matching of the MPS and the DS

The situation is quite analogous to the fracture on the shape of the electric potential at the CPS–MPS interface: on the MPS scale, $\eta = z/\rho_i$, the electric field in the $\varepsilon_{Dm} = (\lambda_D/\rho_i) \to 0$ approximation again runs into a singularity; while on the DS scale, $\xi = z/\lambda_D$, the MPS–DS interface is shifted to the infinity, $\xi \to -\infty$, $(\varphi \to \varphi_s)$, where the electric field according to Eqs. (96) and (99) tends to zero. Therefore, for matching such distinctly different sublayers as the MPS and the DS (the MPS is quasi-neutral, while in the DS the influence of the magnetic field is negligible and the space charge plays an important role), we can repeat the procedure used for matching the CPS with the MPS given above in Sec. IV B. To bridge the MPS and the DS, we again assume the existence of an intermediate region between them. Thanks to the smallness of parameters $\varepsilon_{Dm} = (\lambda_D/\rho_i)$ and $\varepsilon_{Dm} = (\rho_i/\ell)$, both MPS and DS are collisionless in their bulks. The intermediate scale analysis must now account (in lower non-vanishing order) both for the space charge and the finite value of the ion cyclotron radius. Combining Eqs. (83), (84), and (95), we obtain

$$\varepsilon_{Dm}\frac{\partial^2\varphi}{\partial\eta^2} = \int d\mathbf{v}\left\{\bar{f}_i(\varphi, v_x, v_y, v_z; \eta) - \bar{f}_i(\varphi, v_x, v_y, v_z; \overline{\eta})\right\}. \tag{101}$$

We are interested in the case when $\varepsilon_{Dm} \to 0$ and restrict ourselves with analysis of very small region near the sheath edge $\varphi \approx \varphi_s$. Anticipating further that the difference between $\eta(\varphi)$ and $\overline{\eta}(\varphi)$ fades quickly away into the presheath region, for $\overline{\eta}(\varphi)$ we can use the approximation (75). Close to the $\varphi \approx \varphi_s$ region, we can repeat the simplifying procedure, made at the transition from Eq. (92) to Eq. (93); and after integration over velocities, we find

$$\varepsilon_{Dm}\frac{\partial^2\varphi}{\partial\eta^2} = \frac{\alpha}{4\pi}\frac{1}{\sqrt{\varphi-\varphi_m}}\left[\int_{\varphi_m}^{\varphi}\frac{d\varphi'}{\sqrt{\varphi'-\varphi_m}} \times\left\{\frac{\partial\eta(\varphi')}{\partial\varphi'} - \frac{\partial\overline{\eta}(\varphi')}{\partial\varphi'}\right\} - \int_{\varphi_s}^{\varphi}\frac{d\varphi'\overline{\eta}_0(\varphi')}{\sqrt{\varphi'-\varphi_m}}\right]. \tag{102}$$

The intermediate scale variables, as usually,[18] we define in the following way:

$$\begin{aligned} \varphi &= \varphi_s + \delta\cdot w\,,\\ \eta &= \eta_s + b\delta^2\cdot\zeta\,,\\ \overline{\eta} &= \overline{\eta}_s + b\delta^2\cdot\zeta\,, \end{aligned} \tag{103}$$

where b is given by Eq. (76). For φ close to φ_s, Eq. (101) in these variables acquires the form

$$\frac{\partial^2 w}{\partial \zeta^2} = \left[\frac{\alpha}{4\pi} I(\varphi_m) \frac{\delta^5 b^3}{\varepsilon_{Dm}^2(\varphi_s - \varphi_m)}\right] \times \left[\int_{-\infty}^{w} dv\left[\zeta'(v) - \overline{\zeta}'(v)\right] - \int_0^w dv \overline{\zeta}_0'(v)\right], \quad (104)$$

$$\text{with} \quad \overline{\zeta}(v) = \frac{\overline{\eta} - \overline{\eta}_s}{b\delta^2} = -v^2. \quad (105)$$

Choosing

$$\delta = \left[\frac{4\pi}{\alpha I(\varphi_m)} \frac{\varepsilon_{Dm}^2(\varphi_s - \varphi_m)}{\sqrt{2}\, b^2}\right]^{1/5}, \quad (106)$$

we obtain the representation of the Poisson's equation in form

$$\frac{\partial^2 \overline{w}}{\partial \zeta^2} = \zeta + \overline{w}^2, \quad \overline{w} = \sqrt{2}\, w. \quad (107)$$

This intermediate equation represents the Painleve' equation. In obtaining of Eq. (107), the condition of fast fading of the difference $[\zeta(c) - \overline{\zeta}(v)]$ at moving away from the sheath edge inside of the presheath is used. Neglecting the space charge term $\partial^2 \overline{w}/\partial \zeta^2$, we obtain the presheath solution

$$\zeta(\overline{w}) = -\overline{w}^2, \quad (108)$$

which corresponds to Eq. (75). On the other hand, keeping the space charge and neglecting the influence of the magnetic field, represented by the first term in the right-hand side of Eq. (108) [cf. with Eq. (100)], we derive the sheath approximation of the intermediate solution

$$\zeta_{sh}(\overline{w}) = \zeta_0 - \sqrt{3}\, \overline{w}^{-1/2}. \quad (109)$$

Similarity with Eq. (99) is obvious. At $\zeta_{sh}(w) \to \zeta_0$, the approximation w runs into singularity, $w \to \infty$. The place of this singularity $\zeta_0 = 2.97$ is decisive for the consistent "placement" of the wall position.[22] This "placement" is connected with the "eigenvalue" problem of the PWT theory[22] that is not considered here. Using Eqs. (72), (76), and (103) for the characteristic scale-length of the intermediate region, we find

$$l = \left\{\frac{1}{\sqrt{\overline{A}_s}} e^{\varphi_m} F(\overline{A}_s)\right\} \lambda_D^{4/5} \rho^{1/3}. \quad (110)$$

In Fig. 9, the dependences of the full solution $\zeta(w)$ together with its presheath $\overline{\zeta}(w)$ and sheath $\zeta_{sh}(w)$ approximations are shown. Obviously, the function $\zeta(w)$ indeed is a link that provides a smooth transition between the presheath and sheath solutions for small but finite ε_{Dm}.

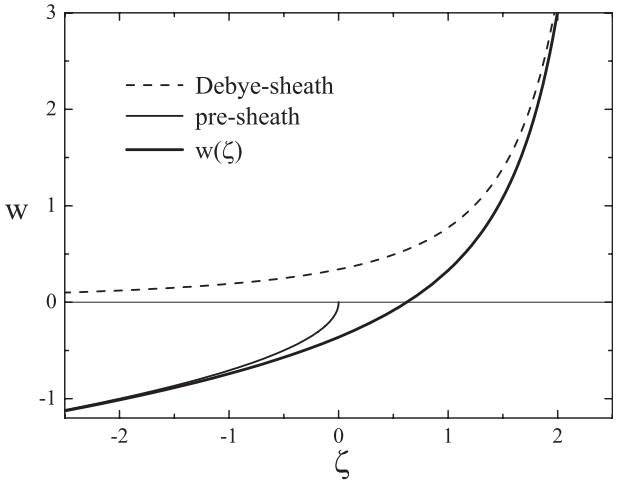

FIG. 9. Intermediate solution.

VI. SUMMARY AND DISCUSSIONS

We have followed the "beaten track" of the MPWT investigation starting our derivations from the CPS and proceeding to the position where the wall boundary condition $\varphi = \varphi_w$ is fulfilled.[13,18] The definition of the wall position is directly connected with solving of the so-called "eigenvalue problem." Physically, this problem reflects the fact that the ion produced rate must be equal to the rate of ion loss onto wall. Obviously, this "plasma balance" condition should be kept.

In this paper, we have provided a kinetic analysis of the MPWT layer under condition that the magnetic field intersects the wall at a small angle $\alpha \ll 1$. Plasma is assumed to be weakly ionized and both the charge exchange collisions of ions with neutrals and ions' creation at the neutrals' ionization by the electron impact are taken into account. The angle α is used as small parameter and the ion distribution function is expanded in series of powers of α, restricting ourselves with its first power.

We have succeeded to reduce the ion kinetic equation in the CPS to the form, which is quite identical to the kinetic equation for the guiding center.[14,15] The total solution of our problem than is determined by the self-consistent potential and the ion distribution function (DF) in the CPS, starting from which all other quantities can be found. Following to the generally accepted procedure, the MPS and the DS entrances are defined as points where the electric field runs into infinity, and fulfillments of the Bohm–Chodura and the Bohm conditions are there confirmed, respectively. The CPS–MPS and the MPS–DS interfaces are used as boundaries that allow to connect the ion DF in the MPS with the DF in the CPS (already known from the solution of the CPS kinetic equation) and further connect the DF in the DS with the DF in the MPS.

The intermediate scale analysis is performed to describe the CPS–MPS and the MPS–DS transitions and to enable smooth matching of these neighboring sublayers.

Here, it should be mentioned that under our conditions:

(i) These quite expectable results can be obtained only in the case, if in the MPS region the ions moving towards the wall do not outline a complete Larmor-circle (see above Sec. IV). They move in the positive z-direction and v_y component of their velocity, starting from the CPS edge (in our coordinate system, see Fig. 2) is negative. Obviously, $v_y = 0$ at the MPS edge, where the electric field (directed along the z-axis to the wall) is infinite. As it is mentioned in Sec. IV, some indication of possibility of such a situation is given in Ref. 19 and also illustrated in Ref. 1, (see p. 99).

(ii) The intermediate scale length l_m for the CPS–MPS transition is rather small. In frame of the A3S, when $\varepsilon_{mc} = (\rho_i/l) \to 0$, the ions assumed to be fastened to the magnetic field-lines, $\rho_i = 0$; and at the transition into the MPS region, they acquire some finite cyclotron radius.

The eigenvalue problem originated from the "plasma balance" and investigations of particle and energy fluxes to the wall we defer to future investigation.

ACKNOWLEDGMENTS

This work has been supported by the European Commission under the Contract of Association between EURATOM and the Austrian Academy of Sciences. It was carried out within the framework of the European Fusion Development Agreement. This work was also supported by the Austrian Science Fund (FWF) under the project P22345-N16. The view and opinions expressed herein do not necessarily reflect those of the European Commission.

APPENDIX: ANALYSYS FOR f_i^-

Below we show that in the case of cold neutrals (cold ion source), the distribution function of ions f_i^-, moving with negative $v_z < 0$ velocity, equals zero.

It is obvious that at the non-reflected wall, where $\varphi = \varphi_w$, or at the DS entrance, where $\varphi = \varphi_s$ and the electric field, directed towards the wall, is infinite, there are no ions with $v_z < 0$ velocity. Hence these points can be employed in the formulation of boundary condition for f_i^-. The system of the characteristic equation for the kinetic equation (5), we represent in the form

$$v_z \frac{dv_x}{dz} = \frac{v_y}{\rho_i} \sin\alpha\,, \tag{A1}$$

$$v_z \frac{dv_y}{dz} = \frac{1}{\rho_i}\{v_z \cos\alpha - v_x \sin\alpha\}\,, \tag{A2}$$

$$v_z \frac{dv_z}{dz} = \frac{\partial\varphi}{\partial z} - \frac{v_y}{\rho_i}\cos\alpha\,, \tag{A3}$$

$$v_z \frac{df_i}{dz} = \frac{1}{\lambda_{cx}}\left\{\delta(\mathbf{v})C(z) - |\mathbf{v}|f_i\right\}. \tag{A4}$$

Contrary to two others one constant of integration, we can find in the explicit form

$$C_z = \{v_z^2 + v_y^2 + v_x^2 - 2\varphi(z)\}^{1/2}\,, \tag{A5}$$

$$C_y = C_y(v_x, v_y, v_z, z)\,, \tag{A6}$$

$$C_x = C_x(v_x, v_y, v_z, z)\,. \tag{A7}$$

It is assumed that one can find also inverse functions

$$v_x = v_x(\mathbf{C}, z)\,, \tag{A8}$$

$$v_y = v_y(\mathbf{C}, z)\,, \tag{A9}$$

$$v_z = \pm\sqrt{C_z^2 - v_x^2(\mathbf{C}, z) - v_y^2(\mathbf{C}, z) + 2\varphi(z)}\,, \tag{A10}$$

where $\mathbf{C} \equiv \{C_x, C_y, C_z\}$. From Eq. (A4) then using relations (A1)–(A10) after straightforward calculations for the · ion distribution function with negative v_z velocity, we obtain

$$\begin{aligned} f_i^-(\mathbf{v},\varphi) = &-\frac{2}{\lambda_{cx}}\int^{\varphi} d\varphi' \frac{dx(\varphi')}{d\varphi'}\delta\left[v_z^2 + v_y^2 + v_x^2 + 2(\varphi' - \varphi)\right] \\ &\times \delta\left\{\left[v_x[\mathbf{C}(\mathbf{v}),\varphi),\varphi'\right]\right\}\cdot\delta\left\{\left[v_y[\mathbf{C}(\mathbf{v}),\varphi),\varphi'\right]\right\} \\ &\cdot C[z(\varphi')]\exp\left\{-\int_{\varphi'}^{\varphi} d\varphi'' \frac{dz(\varphi'')|v\left[\mathbf{C}(v,\varphi),\varphi''\right]|}{d\varphi'' v_z\left[\mathbf{C}(v,\varphi),\varphi'\right]}\right\} \\ &+\bar{\bar{f}}_i^{-}[\mathbf{C}(\mathbf{v},\varphi')] \\ &\times \exp\left\{-\int^{\varphi} d\varphi'' \frac{dz(\varphi'')|v\left[\mathbf{C}(v,\varphi),\varphi''\right]|}{d\varphi'' v_z\left[\mathbf{C}(v,\varphi),\varphi'\right]}\right\}. \end{aligned} \tag{A11}$$

The arbitrary function $\bar{\bar{f}}_i[\mathbf{C}(\mathbf{v},\varphi')]$ should be defined by the boundary conditions

$$f_i^-(\mathbf{v},\varphi_1) = 0\,,\ \text{with}\ \varphi_1 = \varphi_s\,,\ (\text{or}\ \varphi_1 = \varphi_w)\,. \tag{A12}$$

Finally, we find

$$\begin{aligned} f_i^-(v,\varphi_1) = &-\frac{2}{\lambda_{cx}}\int_{\varphi}^{\varphi_1} d\varphi' \frac{dz(\varphi')}{d\varphi'}\times\delta[v_z^2+v_y^2+v_x^2+2(\varphi'-\varphi)] \\ &\times\delta\{[v_x[\mathbf{C}(v),\varphi),\varphi']\}\cdot\delta\{[v_y[\mathbf{C}(v),\varphi),\varphi']\}\cdot C[z(\varphi')] \\ &\times\exp\left\{-\int_{\varphi'}^{\varphi} d\varphi'' \frac{dz(\varphi'')\left|v[\mathbf{C}(v,\varphi),\varphi'']\right|}{d\varphi'' v_z[\mathbf{C}(v,\varphi),\varphi']}\right\}. \end{aligned} \tag{A13}$$

Existence of the first δ-function in the integrand indicates that $f_i^-(\mathbf{v},\varphi_1) = 0$.

[1]P. C. Stangeby, *The Plasma Boundary of Magnetic Fusion Devices* (Institute of Physics Publishing Ltd., Bristol, 2000).
[2]H. Schmitz, K.-U. Riemann, and T. Daube, Phys. Plasmas **3**, 2486 (1996).
[3]T. Daube, K.-U. Riemann, and H. Schmitz, Phys. Plasmas **5**, 117 (1998).
[4]T. Daube and K.-U. Riemann, Phys. Plasmas **6**, 2409 (1999).
[5]R. Chodura, Phys. Fluids **25**, 1628 (1982).
[6]H. Gerhauser and H. A. Claaßen, Contrib. Plasma Phys. **38**, 331 (1998).
[7]S. Devaux and G. Manfredi, Phys. Plasmas **13**, 083504 (2006).
[8]M. Shoucri, H. Gerhauser, and K. H. Finken, Phys. Scr. **75**, 712 (2007).
[9]M. Shoucri, H. Gerhauser, and K. H. Finken, Phys. Plasmas **16**, 103506 (2009).
[10]S. Kuhn, K.-U. Riemann, N. Jelić, D. D. Tskhakaya, Sr., D. Tskhakaya, Jr., and M. Stanojević, Phys. Plasmas **13**, 013503 (2006).
[11]K.-U. Riemann, J. Tech. Phys. **41**, 89 (2000), General Invited Lecture, ICPIG XXIV, Warshaw, 1999, see https://inis.iaea.org/search/searchsinglerecord.aspx?recordsFor=SingleRecord&RN=31064486.
[12]R. N. Franklin, J. Plasma Phys. **78**, 21 (2012).
[13]K.-U. Riemann, Phys. Fluids **24**, 2163 (1981).
[14]T. F. Volkov, in *Reviews of Plasma Physics*, edited by M. A. Leontovich (Consultants Bureau Enterprises, Inc., New York, 1966), Vol. 4, pp. 1–21.
[15]A. Morozov and L. Solov'ev, in *Review of Plasma Physics*, Vol. 2, edited by M. A. Leontovich (Consultants Bureau Enterprises, Inc., New York, 1966), pp. 213–226.
[16]H. Risken, *The Fokker-Planck Equation* (Springer Verlag, Berlin, 1984).
[17]B. I. Braginsckii, in *Review of Plasma Physics*, edited by M. A. Leonktovich (Consulting Bureau, New York, 1965), pp. 205–311.
[18]K.-U. Riemann, Phys. Plasmas **13**, 063508 (2006).
[19]R. H. Cohen and D. D. Ryutov, Phys. Plasmas **5**, 808 (1998).
[20]D. D. Tskhakaya, F. Bint-E-Munir, and S. Kuhn, J. Plasma Phys. **76**, 559 (2010).
[21]D. V. Sivukhin, in *Review of Plasma Physics*, edited by M. A. Leontovich (Consultants Bureau Enterprises, Inc., New York, 1965), Vol. 1, pp. 1–104.
[22]K.-U. Riemann, J. Seebacher, D. D. Tskhakaya, Sr., and S. Kuhn, Plasma Phys. Controlled Fusion **47**, 1949 (2005).